Benthic Foraminiferal Salinity index in marginal-marine environments: A case study from the Holocene Guadalquivir estuary, SW Spain

José Pérez-Asensio, Antonio Rodríguez-Ramírez

▶ **To cite this version:**

José Pérez-Asensio, Antonio Rodríguez-Ramírez. Benthic Foraminiferal Salinity index in marginal-marine environments: A case study from the Holocene Guadalquivir estuary, SW Spain. Palaeogeography, Palaeoclimatology, Palaeoecology, 2020, 560, pp.110021. 10.1016/j.palaeo.2020.110021 . hal-03215057

HAL Id: hal-03215057
https://hal.inrae.fr/hal-03215057

Submitted on 23 Sep 2022

HAL is a multi-disciplinary open access archive for the deposit and dissemination of scientific research documents, whether they are published or not. The documents may come from teaching and research institutions in France or abroad, or from public or private research centers.

L'archive ouverte pluridisciplinaire **HAL**, est destinée au dépôt et à la diffusion de documents scientifiques de niveau recherche, publiés ou non, émanant des établissements d'enseignement et de recherche français ou étrangers, des laboratoires publics ou privés.

Distributed under a Creative Commons Attribution - NonCommercial 4.0 International License

Version of Record: https://www.sciencedirect.com/science/article/pii/S0031018220304697
Manuscript_e214427891a02b315b534482431febc9

Benthic Foraminiferal Salinity index in marginal-marine environments: a case study from the Holocene Guadalquivir estuary, SW Spain

José N. Pérez-Asensio[a,*], Antonio Rodríguez-Ramírez[b]

Authors' addresses:

[a] *CEREGE UM34, Aix Marseille Univ, CNRS, IRD, INRAE, Coll France, 13545 Aix-en-Provence, France*

[b] *Departamento de Ciencias de la Tierra, Universidad de Huelva, Campus de Excelencia Internacional de Medio Ambiente, Biodiversidad y Cambio Global, CEI-Cambio, Avenida de las Fuerzas Armada s/n, 21007 Huelva, Spain*

* Corresponding author; E-mail address: perez@cerege.fr (José N. Pérez-Asensio)

Second author; E-mail address: arodri@uhu.es (Antonio Rodríguez-Ramírez)

Abstract

Here we developed and validated a new Benthic Foraminiferal Salinity (BFS) index from marginal-marine environments by analysing benthic foraminifera from the Holocene Guadalquivir estuary sediments (SW Spain). This index is formulated utilising only four species: *Ammonia tepida* and *Haynesina germanica* with higher tolerance to brackish waters and indicating lower salinity, and *Elphidium translucens* and *Elphidium granosum* indicative of greater marine influence and pointing to higher salinity. Thus, the BFS index is calculated easily and rapidly, and therefore it makes it possible to analyse a higher number of samples in less time. The BFS index values from the studied cores enabled the detailed description of subtle changes in the Guadalquivir estuary restriction during the Holocene. For this purpose, three degrees of salinity, depending on marine influence, were defined: higher (BFS index =

© 2020 published by Elsevier. This manuscript is made available under the CC BY NC user license
https://creativecommons.org/licenses/by-nc/4.0/

0.0-0.4, high marine influence), moderate (BFS index = 0.4-0.7, moderate marine influence), and lower (BFS index = 0.7-1.0, low marine influence). Before 2000 BCE, the estuary was moderately open and well-connected to the Atlantic Ocean. From 2000 BCE, the estuary experienced a greater marine influence, increasing in extension, as a consequence of a sea-level rise and subsidence. Immediately afterwards, it began to experience restriction processes due to southward shoreline progradation related to the growth of littoral spits and sediment supply. From 1400 to 1000 BCE, gradual restriction transformed the open estuary into a semiclosed estuary. A last phase of estuary restriction occurred from 1000 BCE to the present day, leading to the lowest salinity and the highest estuary restriction. Finally, the BFS index was successfully applied in two other marginal-marine environments: a Pleistocene lagoon in northern Italy, and a Pliocene coastal bay in southeastern Spain. The index allowed assessment of the degree of restriction in these different environments, supporting its utility in different regions, environments and timescales.

Keywords: Micropaleontology; Coastal settings; Restriction; Brackish; Quaternary; Europe

1. Introduction

Marginal-marine environments, including estuaries, deltas, fjords, marshes and littoral lagoons, are very sensitive to changes in sea level, tide and wave regime, as well as fluvial dynamics (Chiverrell, 2001; Ybert et al., 2003). These factors play a key role in controlling coastal geomorphological features (spits, dunes, cheniers, marshes, levees, tidal channels), and sedimentary features (sediment supply, sedimentary bodies, sediment infilling), which modify the paleogeography of marginal-marine environments (Gerdes et al., 2003; Durand et al., 2016). Coastal environments occur at the transition between continental fresh waters and

marine normal salinity waters, consequently they are commonly characterised by brackish waters (Rich and Maier, 2015). In coastal environments, the gradual decrease of seawater influence reduces salinity (Guelorget and Perthuisot, 1983, 1992; Debenay, 1995). Thus, marginal-marine environments have lower or higher salinity depending on the lower or higher influence of marine waters, respectively. Salinity is governed by the geomorphological restriction of the coastal environment (i.e., degree of connection to the open sea), which is related to changes in both geomorphological and sedimentary features (Gregoire et al., 2017; Devillers et al., 2019; Haas et al., 2019). Therefore, lower or higher restriction causes higher or lower salinity, respectively.

Benthic foraminifera are widely used for reconstructing paleoenvironmental changes from marginal-marine to deep-sea environments since they are very sensitive to variations in sea level, organic fluxes, oxygen content, salinity and type of substrate (e.g., Alve and Murray, 1999; Jorissen et al., 2007; Di Bella et al., 2008; Martins et al., 2014; Blázquez et al., 2017; Pérez-Asensio et al., 2014, 2017, 2020). In coastal settings, it is well known that benthic foraminiferal distribution and abundance can be influenced by salinity, which is dependent, among other factors, on the geomorphological restriction (Debenay et al., 2006; Barbieri and Vaiani, 2018; Blázquez-Morilla et al., 2019). In fact, benthic foraminifera have been successfully used as proxies of restriction of marginal-marine environments and for developing salinity indices (Debenay, 1995; Hayward et al., 2004; Debenay and Luan, 2006). Previously defined salinity indices (Debenay, 1995; Hayward et al., 2004) are based on complex and time-consuming identification of numerous benthic foraminiferal species, which requires a profound taxonomic knowledge. Hence, it is necessary to create simpler salinity indices based on a low number of species, which would be useful for scientists who are not specialized on benthic foraminiferal taxonomy. Furthermore, identifying fewer species would

imply a faster process for obtaining foraminiferal data, making it possible to analyse more sedimentary records at higher resolution.

The principal objectives of this study were to develop a simple Benthic Foraminiferal Salinity (BFS) index, and to validate it as proxy for different degrees of salinity in marginal-marine environments. For these purposes, we analysed benthic foraminifera from 8 short cores (this study) and two deep cores (Rodríguez-Ramírez et al., 2015), which recovered Holocene sediments from the Guadalquivir estuary (SW Spain) (Figs 1 and 2). The Guadalquivir estuary is an excellent area to assess the performance of our BFS index because its paleogeography, and therefore its connection to the open sea (i.e., marine influence), changed substantially over the Holocene owing to geomorphological and sedimentary processes (Rodríguez-Ramírez et al., 2019). In addition, the applicability of this BFS index was tested in two different environments (lagoon, coastal bay) from other regions (northern Italy, southeastern Spain).

2. Study area: the Guadalquivir estuary

The Guadalquivir estuary (SW Spain) is located in the Gulf of Cadiz (Atlantic Ocean) (Fig. 1). It contains a 180,000 ha freshwater marsh including the Doñana National Park (UNESCOMAB Biosphere Reserve). This estuary has two enclosing spits (Doñana and La Algaida), which are partly covered by active dunes. Both spits protect a wide marsh area behind. This marsh grew without sediment input from the Guadalquivir and convergent rivers because this riverine sediment supply filled in the ancient marine Guadalquivir estuary as finger deltas in a low-energy setting. The growth of the two large littoral spits isolating the estuary and the development of a wide chenier plain favoured this sedimentary process (Rodríguez-Ramírez and Yáñez-Camacho, 2008).

Fluvial regime, tidal inflow, wave action, and drift currents controlled the Guadalquivir estuary hydrodynamics. The Guadalquivir river is the largest river draining SW Spain and the principal source for fluvial sediments in the southwestern Spanish coast. This river has a mean annual discharge of 164 m^3/s, with winter spates that can easily exceed 5000 m^3/s (Vanney, 1970). At the river mouth in the period from 1997 to 2003, the average tidal range was 2 m with a maximal tidal range of 3.86 m (Spanish Ministry of Fomento, 2005). Accordingly, the coastline is mesotidal, semidiurnal.

The wave regime is directly related to the prevailing SW winds, with 22.5% of the days of the year with SW winds (Rodríguez-Ramírez et al., 2003). Overall, the wave regime has medium-to-low energy, with waves normally <0.6 m high (data of Departamento de Clima Marítimo). Atlantic cyclones are frequent during winter and they foster strong SW winds, generating significant erosion in the coastline (Rodríguez-Ramírez et al., 2003). Most of the wave fronts approach obliquely the coastline generating longshore currents that transport sand from the Portuguese coast to Spanish nearshore areas.

3. Methodology

3.1. Lithostratigraphy

We studied the sedimentary sequences and facies from 8 short cores (<3 m): S6, LB, AR, AA, VT, VAc, VAli.2 and VAli.1 (Table 1). The cores were drilled with a 4-cm-diameter Eijkelkamp gouge, an 8-cm-diameter drill, and trenches. We also analysed previously published sedimentary records from two long cores: S7 and S11 (Table 1) (Rodríguez-Ramírez et al., 2015). Grain-size analyses were performed using conventional sieving for fractions >2 mm, and a Malvern Mastersizes 2000 laser diffraction particle

analyser for smaller particle sizes between 2 mm and 2 µm. Shepard's sediment classification (Shepard, 1954) was applied to grain-size results in order to describe sediment texture, including sand, silt and clay fractions.

3.2. Radiocarbon dating

Eight new radiocarbon dates were measured on mollusc shells at the laboratories of Centro Nacional de Aceleradores (Seville, Spain) and Accium BioSciences Accelerator Mass Spectrometry Lab (Seattle, USA) (Table 2, Fig. 2). Other 14 radiocarbon dates from previous studies (Rodríguez-Ramírez et al., 2014, 2015, 2016) were used in this work (Table 2, Fig. 2). Calibration of radiocarbon data was conducted by means of CALIB 7.10 software (Stuiver and Reimer, 1993) and the calibration dataset of Reimer et al. (2013). Uncertainties of the calibrated ages are expressed as 2σ errors. The reservoir effect was corrected using the ΔR values recommended by Soares (2015). This author suggested a ΔR value of −108 ± 31 ^{14}C yr for the late Holocene on the Andalusian coast of the Gulf of Cadiz; excluding the years 4400–4000 ^{14}C yr BP, for which he recommended a ΔR value of +100 ± 100 ^{14}C yr. In the interval from 4000 to 2000 ^{14}C yr BP, lack of data impedes pinpointing the most recent time boundary to which the +100 ± 100 ^{14}C yr ΔR value can be extended. In spite of this problem, we decided to tentatively extend it to the middle year 3000 ^{14}C yr BP.

3.3. Micropaleontology

A total of 45 sediment samples (~50 g) was wet-sieved over a 63 µm mesh and dried in an oven at 40°C. Samples were thoroughly split using a microsplitter so as to obtain sub-samples. Then, theses sub-samples were dry-sieved over a 125 µm mesh, and at least 300 benthic foraminifera were carefully counted and identified to the species level (Loeblich and

146 Tappan, 1987; Milker and Schmiedl, 2012; Pérez-Asensio et al., 2012). Raw counts were
147 transformed into relative abundances (%). Q-mode principal component analysis (PCA) was
148 carried out on all samples from the short and long cores using the software OriginPro 2020.
149 All species were included in the analysis. The PCA allowed to establish benthic foraminiferal
150 assemblages and to infer environmental factors controlling these assemblages (Parker and
151 Arnold, 1999; Milker et al., 2009) (Table 3, Fig. 3).

152 In this study, we developed a new Benthic Foraminiferal Salinity (BFS) index for
153 assessing the salinity changes in marginal-marine environments (e.g., estuaries, lagoons,
154 marshes). This BFS index is based on the distribution of some of the dominant benthic
155 foraminiferal species found in the Holocene Guadalquivir estuary sediments (see discussion
156 section 5.2).

157

158 **4. Results**

159

160 *4.1. Lithostratigraphy and chronology of the deep cores: S7 and S11*

161 The sedimentary sequence and chronology of deep cores S7 and S11 are described in
162 detail in prior studies (Jiménez-Moreno et al., 2015; Rodríguez-Ramírez et al., 2015).

163 The core S11 is 18 m long and its lower part (18 to 12.5 m) consists of a Pleistocene
164 marsh sequence of mostly greyish ochre clayey silts (Fig. 2). From 12.5 m to the top, the
165 Holocene sequence is dominated by grey-greenish clayey silts, with three intercalated sandy
166 layers at around 12, 9, and 7 m (Fig. 2). These sandy layers have been interpreted as Extreme
167 Wave Events (EWEs) (Rodríguez-Ramírez et al., 2015) occurring at ca. 2270, 1657, and
168 1421 BCE, respectively (Fig. 2).

169 The sedimentary sequence in core S7 is 9 m long, beginning with aeolian sands (9-
170 8.75 m) from the El Abalario Dune Formation (Fig. 2). Holocene greyish ochre clayey silts
171 dominate from 8.75 to the core top. Three sandy layers related to EWEs appear at around 8.5,
172 5.5, and 2.5 m, being dated at ca. 1983, 1657, and 1142 BCE, respectively (Fig. 2).

173

174 *4.2. Lithostratigraphy and chronology of the short cores: S6, LB, AR, AA, VT, VAc, VAli.2*
175 *and VAli.1*

176 The core S6 recovered 1.5 m of sediments, with clayey silts at the lower part and
177 sands at the upper part (Fig. 2). Sandy facies were dated at 2439 BCE. The core LB is 1.25 m
178 long and it mostly consists of clayey silts. At around 0.9 m, a shelly layer appears with an age
179 of 52 ACE. The sediment record of core AR includes 1.25 m of clayey silts with a shelly
180 layer at around 0.5 m (232 BCE). The core AA has a length of 1.25 m and it is composed of
181 clayey silts with an intercalated shelly layer at around 0.4 m (304 BCE). In the 2-m long core
182 VT, clayey silts range from 2 to 1.25 m, and a thick shelly layer, dated ca. 1304-1151 BCE,
183 occurs towards the top. The core VAc recovered 2 m of sands dated at ca. 1659-1408 BCE.
184 The VAli.2 core (1.75 m long) shows clayey silts in the lower part (1.75-1 m) and a shelly
185 layer (ca. 2205-2022 BCE) in the upper part (1-0 m). The VAli.1 core encompasses 1.4 m of
186 sands dated ca. 2230-2190 BCE.

187

188 *4.3. Benthic foraminiferal data*

189 The Q-mode principal component analyses (PCA) considering all samples from the
190 studied cores yielded three assemblages (PC-1 to 3), explaining 67.8%, 23.3% and 4.2% of
191 the total variance, respectively (Table 3). The benthic foraminiferal assemblage from the PC-
192 1 is dominated by *Ammonia tepida* with *Haynesina germanica*, *Elphidium translucens* and

193 *Elphidium granosum* as secondary species. In the assemblage from the PC-2, *H. germanica* is
194 the unique and dominant species. The assemblage from the PC-3 has *Triloculina trigonula* as
195 dominant species, and includes several additional taxa such as *Ammonia beccarii*,
196 *Quinqueloculina seminula*, *Miliolinella* sp., *Quinqueloculina* sp., *Triloculina* sp.,
197 *Quinqueloculina vulgaris*, and *Quinqueloculina laevigata*. All taxa from this assemblage
198 (PC-3) are marine species transported into the estuary by EWEs (Rodríguez-Ramírez et al.,
199 2015). Consequently, they will not be considered to assess the salinity conditions of the
200 Guadalquivir estuary.

201 The relative abundances of the dominant and secondary taxa from the PC-1 and PC-2
202 assemblages are shown in Fig. 2. In the S11 core, *H. germanica* shows fairly low values
203 (<20%) from the base to 4.5 m (Fig. 2). Then, it increases until reaching maximal values
204 (80%) from 3 to 2 m, and it decreases upwards. *A. tepida* relative abundance rises from the
205 bottom to 5 m, it diminishes from 5 to 2 m, and it rises towards the core top. *E. translucens*
206 has higher values in the lower part of the core (12.5-5 m), and shows its highest abundance
207 (~25%) at 6.5 m (Fig. 2). In the S7 core, *H. germanica* has very low abundance (<10%) from
208 the core base to 2.5 m, and gradually increasing abundances from 2.5 m towards the core top.
209 *A. tepida* shows considerably high values (40-60%) from the core base to 3.5 m, and it
210 declines upwards. Both *E. translucens* and *E. granosum* have higher abundance (10-35%)
211 from the core bottom to 3.5 m than in the upper part of the core (3.5-1 m), where they
212 virtually disappear. In core S6, both *A. tepida* and *H. germanica* are very abundant (~50%) in
213 interval from 1.25 to 0.75 m, whereas *E. translucens* has very low abundance (<6%) in the
214 same interval. The core LB shows opposite trends for *H. germanica* and *A. tepida*, with
215 higher values of *H. germanica* (~65%) and lower values of *A. tepida* (~25%) from 1.1 to 0.4
216 m. In the interval from 0.4 to 0.2 m, *A. tepida* increases while *H. germanica* decreases. *E.*
217 *translucens* and *E. granosum* have very low abundances (<10%) along the core. In the AR

and AA cores, *H. germanica* is very abundant (80-90%), whereas *A. tepida*, *E. translucens* and *E. granosum* show low abundances (<15%) in both cores. The cores VT and VAc have high values of *A. tepida* (50-65%), and low values of *H. germanica* (10-20%). *E. translucens* and *E. granosum* have low values (<15%), decreasing upwards. In the core VAli.2, *A. tepida* shows higher abundances (40-60%), whereas *H. germanica* shows lower abundances (15-30%). Both species abundances drop towards the core top. *E. translucens* and *E. granosum* have very low abundances (<10%). The core VAli.1 has high abundance of *A. tepida* (30-50%), which diminishes upwards. In this core, *H. germanica* and *E. translucens* have very low abundances (<10%).

5. Discussion

5.1. Ecology of benthic foraminiferal species from marginal-marine environments

The two most significant assemblages (PC-1 and PC-2) include *Ammonia tepida*, *Haynesina germanica*, *Elphidium translucens* and *Elphidium granosum* (Table 3). *A. tepida* is a euryhaline species tolerating brackish waters (Murray, 2006; Blázquez and Usera, 2010; Pérez-Asensio and Aguirre, 2010). This species can thrive in environments with low oxygen content and/or high organic matter fluxes (Martins et al., 2013; Wukovits et al., 2018). According to Jorissen et al. (2018), *A. tepida* is a second-order opportunist, which highly increases when organic matter supply is maximal. The species *H. germanica* is also a euryhaline foraminifera resisting a wide range of salinities (Murray, 2006; Blázquez and Usera, 2010). This species can inhabit low oxygenated settings, and it is abundant in sediments with highly variable organic matter content (Alve and Murray, 1999; Martins et al., 2013). *H. germanica* is a third-order opportunist that increases its abundance due to higher

organic matter supply, but it is absent when organic matter input is maximal (Jorissen et al., 2018). *E. translucens* is common in euryhaline marginal-marine environments (Murray, 2006; Pérez-Asensio and Aguirre, 2010). As other *Elphidium* species, it is less tolerant to low oxygen conditions than species from the *Ammonia* group (Sen Gupta and Platon, 2006). This species is an indifferent species, which do not increase with organic matter fluxes, and disappears if organic matter input is high (Jorissen et al., 2018). *E. granosum* is abundant in marginal-marine environments, and tolerates wide salinity changes (euryhaline) (Vaiani, 2000; Curzi et al., 2006; Pérez-Asensio and Aguirre, 2010). This species can benefit from high organic matter fluxes as long as oxygen content is not very low (Jorissen, 1988). It is considered a third-order opportunist, rising its abundance as a response to higher organic matter supply, yet disappearing with maximum organic matter enrichment (Jorissen et al., 2018).

5.2. Development of the Benthic Foraminiferal Salinity index

Benthic foraminiferal assemblages from the Holocene sediments recovered in the Guadalquivir estuary area allowed to developed a new Benthic Foraminiferal Salinity (BFS) index. As mentioned above, the most important species (*A. tepida*, *H. germanica*, *E. translucens*, *E. granosum*) are euryhaline species (i.e., tolerating wide salinity variations). These species can inhabit marginal-marine environments with brackish waters such as estuaries, marshes and littoral lagoons (Debenay, 1995; Ruiz et al., 2005; Murray, 2006; Blázquez and Usera, 2010; Pérez-Asensio and Aguirre, 2010). Marginal-marine environments can have different degrees of salinity related to higher or lower influence of marine waters. This depends on their paleogeography, geomorphology, and wave and tide regimes (Pethick, 1984; Pérez-Ruzafa et al., 2019). The comparison of the Principal

Component (PC) scores of species belonging to the euryhaline assemblage PC-1 shows that *A. tepida* and *H. germanica* present higher scores than *E. translucens* and *E. granosum* (Fig. 3, Table 3). This suggests that higher scores of PC-1 indicate less salinity since *A. tepida* and *H. germanica* have high tolerance to brackish conditions (i.e., less marine influence), and can inhabit inner estuaries (Alve and Murray, 1994; Debenay and Guillou, 2002; Ruiz et al., 2004, 2005; Murray, 2006; Mojtahid et al., 2016). On the contrary, *E. translucens* and *E. granosum*, as other noncarinate elphidiids, occur in outer estuaries with important marine influence (Ruiz et al., 2005; Mojtahid et al., 2016). Considering the environmental conditions indicated by *A. tepida*, *H. germanica*, *E. translucens* and *E. granosum* in the Guadalquivir estuary, a new Benthic Foraminiferal Salinity (BFS) index has been developed for reconstructing salinity changes within overall hyposaline conditions. Consequently, the BFS index was established using the relative abundances of *A. tepida* and *H. germanica* as indicative of lower salinity, and *E. translucens* and *E. granosum* as indicative of higher salinity. The expression of the BFS index is:

$$\text{BFS index} = (\%\ A.\ tepida + H.\ germanica) / (\%\ A.\ tepida + H.\ germanica + E.\ translucens + E.\ granosum)$$

The BFS index varies from 0 (higher salinity) to 1 (lower salinity), therefore higher values of the index indicate lower salinities, and vice versa. We posit that this BFS index may be a powerful tool to qualitatively reconstruct salinity changes and geomorphological restriction in present-day and ancient marginal-marine environments such as estuaries, marshes and lagoons. Similar indices for reconstructing salinity fluctuations were developed previously (Debenay, 1995; Hayward et al., 2004), but they were based on the relative abundances of a high number of species from benthic foraminiferal assemblages. The calculation of these indices is more complex since it is necessary to perform taxonomic identifications of a high number of species. In contrast, our BFS index requires the

identification of a very low number of species, which makes the application of this index easy and rapid. As a result, a profound taxonomic knowledge is not needed to use the index, and a higher number of samples can be analysed more rapidly.

5.3. Holocene paleoenvironmental evolution of the Guadalquivir estuary

The Holocene paleoenvironmental evolution of the Guadalquivir estuary was unravelled using the new Benthic Foraminiferal Salinity (BFS) index based on dominant benthic foraminiferal species. In order to assess past paleoenvironmental changes in detail, we use three degrees of salinity based on Debenay (1995) (Fig. 4): 1) higher salinity (BFS index = 0.0-0.4, high marine influence), 2) moderate salinity (BFS index = 0.4-0.7, moderate marine influence), 3) lower salinity (BFS index = 0.7-1.0, low marine influence).

In the interval before 2000 BCE, the salinity is higher and moderate in cores at a SW position, near the Atlantic Ocean (cores S7, S11) (Figs 2 and 4). Therefore, this area was well connected with the open sea during this interval. The core S6, located north of cores S7 and S11, records lower salinity, suggesting proximity of paleocoast towards the N. In the eastern area, the cores V.Ali1 and V.Ali2 show high BFS index values (lower salinity) confirming that paleocoast was in a northern position. The morphostratigraphic relationship between V.Ali1, sandy chenier, and V.Ali2, shelly chenier, reflects the progressive restriction of the estuary in the eastern area, before 2000 BCE. These data indicate an overall wide and moderately open paleoestuary, with an efficient connection to the Atlantic Ocean, although the processes of restriction and sedimentary infilling are evident, especially in the east. In this moderately open estuary, marine influence was high as shown by presence of marine fauna transported by tidal flows (Ruiz et al., 2005; Rodríguez-Ramírez et al., 2015).

From 2000 to 1400 BCE approximately, the estuary experimented a greater connection with the sea with higher marine influence, principally in distal areas, as a result of subsidence processes, sea-level rise and tsunamis (Rodríguez-Ramírez et al., 2014, 2015). This is especially visible in the nature of sandy sediments, corresponding to a small spit or sandy chenier, in the upper part of core S6, although without foraminiferal remains, due to intense rework of the sands (Rodríguez-Ramírez et al., 2015). At the SW area (cores S7 and S11), this stronger marine influence is evident by the decrease in BFS index from high to moderate values until 1400 BCE, approximately (Figs 2 and 4). In the eastern area, the lower part of cores VT and VAc show high BFS index values (lower salinity) confirming that the paleocoast was in a more northern position. The absence of sedimentary record at core V.Ali1 might suggest that the NE area was already emerged.

In the interval from 1400 to 1000 BCE, the cores S7 and S11 show increasing BFS index values upwards, and the core S6 could be emerged. This indicates a southward shoreline progradation in the western area. Cores VT and VAc present high BFS index values during the entire interval. The locations of cores V.Ali2 and V.Ali1 were probably emerged. We interpreted the interval from 1400 to 1000 BCE as a phase of estuary restriction leading to a smaller estuary with less connection to the open sea. This interval coincides with the transition from an open estuary to a semiclosed estuary dated at 1200 BCE (Rodríguez-Ramírez et al., 2015). Growth of littoral spits in the river mouth and sedimentary infilling of the estuary may account for this gradual restriction (Rodríguez-Ramírez and Yáñez-Camacho, 2008).

The interval from 1000 BCE to present day is characterised by high BFS index values (lower salinity) in the central area (cores LB, AR, AA) (Figs 2 and 4). In the western area, cores S7 and S11 also show high BFS index values. The location of core S6 was likely emerged during this interval. The eastern area displays high BFS index values in core VT

339 pointing to high geomorphological restriction for the entire interval. In addition, the locations
340 of cores VAc, V.Ali2, and V.Ali1 were surely emerged, suggesting a southward migration of
341 the paleocoast. Therefore, this interval (1000 BCE-present) can be interpreted as a last phase
342 of estuary restriction representing the lowest salinity and highest estuary restriction in the
343 Holocene Guadalquivir estuary evolution.

344

345 *5.4. Application of the BFS index to other regions*

346 In order to test the applicability of the Benthic Foraminiferal Salinity (BFS) index to
347 other regions, we calculated the index in one sediment core (core 223 S12) and one
348 stratigraphic section (Rambla de la Sepultura (RS) section) from two different regions and
349 environments (Figs 1 and 5): 1) a Pleistocene lagoon in northern Italy (Barbieri and Vaiani,
350 2018); and 2) a Pliocene coastal bay in southeastern Spain (Pérez-Asensio and Aguirre,
351 2010). We selected these two regions because, together with the Guadalquivir estuary, they
352 are representative of the most common types of marine-marginal environments. The
353 Pleistocene lagoon from N Italy was a brackish lagoon environment (Barbieri and Vaiani,
354 2018). Benthic foraminiferal assemblages from lagoonal sediments from core 223 S12 were
355 dominated by *Ammonia parkinsoniana* and intermediate *Ammonia tepida–Ammonia*
356 *parkinsoniana* forms, with secondary taxa including *Haynesina germanica*, *Aubignyna*
357 *perlucida*, *Ammonia tepida*, and *Cribroelphidium granosum* (Barbieri and Vaiani, 2018). The
358 Pliocene coastal bay from SE Spain was a restricted coastal bay with coral banks, which was
359 filled with terrigenous sediments of prograding fan deltas (Pérez-Asensio and Aguirre, 2010).
360 In the RS section from this sheltered bay, benthic foraminiferal assemblages were mainly
361 characterised by species from the genus *Ammonia* (*A. beccarii*, *A. tepida*, *A. inflata*) and
362 noncarinate *Elphidium* species (*E. translucens*, *E. granosum*) (Pérez-Asensio and Aguirre,

2010). BFS index values from these different locations and environments were compared with the BFS index values from core S7 (Fig. 5). In this core from the Holocene Guadalquivir estuary, BFS index increased from low to high values in the lower part of the core, indicating progressive restriction. The BFS index values decreased in the middle part of the core, indicating better connection to the Atlantic Ocean. Finally, values increased from moderate to high values, marking the final phase of estuary restriction. In the core 223 S12 from the Pleistocene lagoon of northern Italy, BFS index was overall high along the core, except for two samples at 163.2 and 161.9 m (Fig. 5). These values suggest that this marginal-marine environment was highly restricted, and only experienced better connection to the sea episodically. This interpretation is consistent with a brackish lagoon environment with minor environmental fluctuations related to both freshwater and marine water inputs (Barbieri and Vaiani, 2018). The BFS index values from the Pliocene coastal bay from southeastern Spain increased gradually from low to high values along the RS section. This upward decrease in salinity is in good agreement with a brackish environment that was progressively restricted due to the progradation of fan deltas (Pérez-Asensio and Aguirre, 2010).

After applying the BFS index to two other regions, we propose that our index can be successfully applied to different regions, environments and timescales. This is very feasible because the four species used to calculate the index are widespread in marginal-marine environments around the world. To calculate the index, it is only necessary the presence of *A. tepida* or *H. germanica*, and *E. translucens* or *E. granosum*. Additionally, if *E. translucens* and *E. granosum* are not found, other noncarinate elphidiids with similar ecological requirements might be used (e.g. *Cribroelphidium excavatum*) (Mojtahid et al., 2016). Accordingly, only two to four species are needed to be identified, making the application of the index to other regions simple and fast.

6. Conclusions

Benthic foraminiferal distribution and abundance from the Holocene Guadalquivir estuary are controlled by the degree of salinity. This relationship allowed us to develop a simple Benthic Foraminiferal Salinity (BFS) index based on four benthic foraminiferal species (*A. tepida*, *H. germanica*, *E. translucens*, *E. granosum*). Since the BFS index is based on the identification of a very low species number, it is easy to calculate, even for scientists lacking a profound knowledge on benthic foraminiferal taxonomy. The low number of species to be identified also permits to calculate the BFS index rapidly, which is a great advantage for large-scale studies involving a high number of samples and sites.

The BFS index has allowed us to describe reliably the Holocene paleoenvironmental evolution of the Guadalquivir estuary with great detail, validating the index as proxy for different degrees of salinity, and therefore marine influence. We used three degrees of salinity (higher = 0.0-0.4, moderate = 0.4-0.7, lower = 0.7-1.0), which help us to differentiate subtle changes in geomorphological restriction during the Holocene. According to the BFS index values, the Holocene paleoenvironmental evolution of the estuary had four distinct phases: 1) wide and moderately open estuary (> 2000 BCE), with high connection to the Atlantic Ocean allowing the entrance of transported marine fauna; 2) (2000-1400 BCE) expansion of estuary due to sea-level rise and subsidence; 3) a phase of estuary restriction (1400-1000 BCE), with southward shoreline progradation related to spits growth and sedimentary infilling, which coincides with the transition from open to semiclosed estuary; 4) last phase of estuary restriction (1000 BCE-present day), with the lowest salinity and highest estuary restriction.

Our BFS index can also be applied to other regions, environments and timescales, identifying only two to four species (*A. tepida* or *H. germanica* + *E. translucens* or *E.*

412 *granosum*). This means the index is simple and rapid to calculate, and useful for qualitatively
413 reconstructing salinity changes in worldwide marginal-marine environments from different
414 time periods.

415 **Declaration of competing interest**

416 The authors state that they have no competing financial or personal interests that
417 could represent a conflict of interest.

418

419 **Acknowledgments**

420 We are very grateful to the Editor-in-Chief, Professor Thomas J. Algeo, for his
421 comments and the editorial handling of this manuscript. We also would like to thank two
422 anonymous reviewers for their very constructive comments, which greatly improved this
423 manuscript. We thank the Fundación Caja de Madrid, Fundación Doñana 21, Ayuntamiento
424 de Hinojos, Fundación FUHEM, Estación Biológica de Doñana (EBD), Espacio Natural de
425 Doñana (END), Instituto Andaluz del Patrimonio Histórico (IAPH), Delegación de Cultura of
426 Junta de Andalucía in Huelva, and Organismo Autónomo Parques Nacionales of Ministerio
427 de Medio Ambiente y Medio Rural y Marino for their support of the Hinojos Project.
428 Additional support by Junta de Andalucía to the Research Groups RNM-276 and RNM-190
429 is also acknowledged. JNPA is member of the Research Groups RNM-190 (Junta de
430 Andalucía), GRC Geociències Marines (2017 SGR 315, Generalitat de Catalunya), and
431 Climate Research Group (CEREGE).

432

433 **References**

Alve, E., Murray, J.W., 1994. Ecology and taphonomy of benthic foraminifera in a temperate mesotidal inlet. J. Foramin. Res. 24, 18–27. http://dx.doi.org/10.2113/gsjfr.24.1.18.

Alve, E., Murray, J.W., 1999. Marginal marine environments of the Skagerrak and Kattegat: a baseline study of living (stained) benthic foraminiferal ecology. Palaeogeogr. Palaeoclimatol. Palaeoecol. 146, 171–193. https://doi.org/10.1016/S0031-0182(98)00131-X

Barbieri, G., Vaiani, S.C., 2018. Benthic foraminifera or Ostracoda? Comparing the accuracy of palaeoenvironmental indicators from a Pleistocene lagoon of the Romagna coastal plain (Italy). J. Micropalaeontol. 37, 203–230. https://doi.org/10.5194/jm-37-203-2018

Blázquez, A.M., Usera, J., 2010. Palaeoenvironments and Quaternary foraminifera in the Elx coastal lagoon (Alicante, Spain). Quat. Int. 221, 68–90. https://doi.org/10.1016/j.quaint.2009.06.033

Blázquez, A.M., Rodríguez-Pérez, A., Torres, T., Ortiz, J.E., 2017. Evidence for Holocene sea level and climate change from Almenara marsh (western Mediterranean). Quat. Res. 88, 206–222. https://doi.org/10.1017/qua.2017.47

Blázquez-Morilla, A.M., Rodríguez-Pérez, A., Sanjuán-Lamata, D., 2019. Palaeoenvironmental evolution from the early Holocene to the present of the Almenara marsh (western Mediterranean). Sci. Mar. 82, 257–268. https://doi.org/10.3989/scimar.04853.07A

Chiverrell, R.C., 2001. A proxy record of late Holocene climate change from May Moss, northeast England. J. Quaternary Sci. 16, 9–29. https://doi.org/10.1002/1099-1417(200101)16:1<9::AID-JQS568>3.0.CO;2-K

Curzi, P.V., Dinelli, E., Ricci Lucchi, M., Vaiani, S.C., 2006. Palaeoenvironmental control on sediment composition and provenance in the late Quaternary deltaic successions: a

459 case study from the Po delta area (Northern Italy). Geological Journal 41, 591–612.
460 https://doi.org/10.1002/gj.1060
461 Debenay, J.-P., 1995. Can the confinement index (calculated on the basis of foraminiferal
462 populations) be used in the study of coastal evolution during the quaternary? Quat.
463 Int. 29–30, 89–93. https://doi.org/10.1016/1040-6182(95)00001-Y
464 Debenay, J.-P., Guillou, J.-J., 2002. Ecological transitions indicated by foraminiferal
465 assemblages in paralic environments. Estuaries 25, 1107–1120.
466 http://dx.doi.org/10.1007/BF02692208
467 Debenay, J.-P., Luan, B.T., 2006. Foraminiferal assemblages and the confinement index
468 as tools for assessment of saline intrusion and human impact in the Mekong Delta
469 and neighbouring areas (Vietnam). Rev. Micropaleontol. 49, 74–85.
470 https://doi.org/10.1016/j.revmic.2006.01.002
471 Debenay, J.-P., Bicchi, E., Goubert, E., Armynot du Châtelet, E., 2006. Spatio-temporal
472 distribution of benthic foraminifera in relation to estuarine dynamics (Vie estuary,
473 Vendée, W France). Estuar. Coast. Shelf Sci. 67, 181–197.
474 https://doi.org/10.1016/j.ecss.2005.11.014
475 Devillers, B., Bony, G., Degeai, J.-P., Gascò, J., Lachenal, T., Bruneton, H., Yung, F.,
476 Oueslati, H., Thierry, A., 2019. Holocene coastal environmental changes and human
477 occupation of the lower Hérault River, southern France. Quat. Sci. Rev. 222, 105912.
478 https://doi.org/10.1016/j.quascirev.2019.105912
479 Di Bella, L., Casieri, S., Carboni, M.G., 2008. Late Quaternary paleoenvironmental
480 reconstruction of the Tremiti structural high (Central Adriatic Sea) from benthic
481 foraminiferal assemblages. Geobios 41, 729–742.
482 https://doi.org/10.1016/j.geobios.2008.06.001

Durand, M., Mojtahid, M., Maillet, G.M., Proust, J.-N., Lehay, D., Ehrhold, A., Barré, A., Howa, H., 2016. Mid- to late-Holocene environmental evolution of the Loire estuary as observed from sedimentary characteristics and benthic foraminiferal assemblages. J. Sea Res. 118, 17–34. https://doi.org/10.1016/j.seares.2016.08.003

Gerdes, G., Petzelberger, B.E.M., Scholz-Böttcher, B.M., Streif, H., 2003. The record of climatic change in the geological archives of shallow marine, coastal, and adjacent lowland areas of Northern Germany. Quat. Sci. Rev. 22, 101–124. https://doi.org/10.1016/S0277-3791(02)00183-X

Gregoire, G., Le Roy, P., Ehrhold, A., Jouet, G., Garlan, T., 2017. Control factors of Holocene sedimentary infilling in a semi-closed tidal estuarine-like system: the bay of Brest (France). Mar. Geol. 385, 84–100. https://doi.org/10.1016/j.margeo.2016.11.005

Guelorget, O., Perthuisot, J.P., 1983. Le domaine paralique. Expressions géologiques, biologiques et économiques du confinement. Trav. Lab. Gdol. ENS Paris, 16, 1–136.

Guelorget, O., Perthuisot, J.P., 1992. The Paralic Realm. Biological organization and functioning. Vie Milieu 42, 215–251.

Haas, T. de, Valk, L. van der, Cohen, K.M., Pierik, H.J., Weisscher, S.A.H., Hijma, M.P., Spek, A.J.F. van der, Kleinhans, M.G., 2019. Long-term evolution of the Old Rhine estuary: Unravelling effects of changing boundary conditions and inherited landscape. Depositional Rec. 5, 84–108. https://doi.org/10.1002/dep2.56

Hayward, B.W., Scott, G.H., Grenfell, H.R., Carter, R., Lipps, J.H., 2004. Techniques for estimation of tidal elevation and confinement (~salinity) histories of sheltered harbours and estuaries using benthic foraminifera: examples from New Zealand. Holocene 14, 218–232. https://doi.org/10.1191/0959683604hl678rp

Jiménez-Moreno, G., Rodríguez-Ramírez, A., Pérez-Asensio, J.N., Carrión, J.S., López-Sáez, J.A., Villarías-Robles, J.J., Celestino-Pérez, S., Cerrillo-Cuenca, E., León, Á.,

508 Contreras, C., 2015. Impact of late-Holocene aridification trend, climate variability
509 and geodynamic control on the environment from a coastal area in SW Spain.
510 Holocene 25, 607–617. https://doi.org/10.1177/0959683614565955
511 Jorissen, F.J., 1988. Benthic foraminifera from the Adriatic Sea; principles of phenotypic
512 variation. Utrecht Micropaleontology Bulletin 37, 1–176.
513 Jorissen, F.J., Fontanier, C., Ellen, T., 2007. Paleoceanographical proxies based on deep-sea
514 benthic foraminiferal assemblage characteristics. In: Hillaire-Marcel, C., De Vernal,
515 A. (Eds.), Developments in Marine Geology, Vol. 1. Elsevier, Amsterdam, pp. 263–
516 325.
517 Jorissen, F.J., Nardelli, M.P., Almogi-Labin, A., Barras, C., Bergamin, L., Bicchi, E., El
518 Kateb, A., Ferraro, L., McGann, M., Morigi, C., Romano, E., Sabbatini, A.,
519 Schweizer, M., Spezzaferri, S., 2018. Developing Foram-AMBI for biomonitoring in
520 the Mediterranean: species assignments to ecological categories. Mar.
521 Micropaleontol. 140, 33–45. https://doi.org/10.1016/j.marmicro.2017.12.006.
522 Loeblich Jr., A.R., Tappan, H., 1987. Foraminiferal Genera and Their Classification. 2
523 Volumes. 1: 970 pp.; 2: 213 pp. 847 pls. Van Reinhold Company, New York.
524 Martins, V.A., Frontalini, F., Tramonte, K.M., Figueira, R.C.L., Miranda, P., Sequeira, C., et
525 al., 2013. Assessment of the health quality of Ria de Aveiro (Portugal): Heavy metals
526 and benthic foraminifera. Mar. Pollut. Bull. 70, 18–33.
527 https://doi.org/10.1016/j.marpolbul.2013.02.003
528 Martins, V.A., Frontalini, F., Rodrigues, M.A., Dias, J.M.A., Laut, L.L.M., Silva, F.S.,
529 Clemente, I.M.M.M., Reno, R., Moreno, J., Sousa, S.M.S., Zaaboub, N., El Bour, M.,
530 Rocha F., 2014. Foraminiferal Biotopes and their Distribution Control in Ria de

Aveiro (Portugal): a multiproxy approach. Environ. Monit. Assess. 186, 8875–8897. https://doi.org/10.1007/s10661-014-4052-7

Milker, Y., Schmiedl, G., Betzler, C., Römer, M., Jaramillo-Vogel, D., Siccha, M., 2009. Distribution of recent benthic foraminifera in shelf carbonate environments of the Western Mediterranean Sea. Mar. Micropaleontol. 73, 207–225. https://doi.org/10.1016/j.marmicro.2009.10.003

Milker, Y, Schmiedl, G, 2012. A taxonomic guide to modern benthic shelf foraminifera of the western Mediterranean Sea. Palaeontol. Electron. 15, 16A, 134 p. palaeo-electronica.org/content/2012-issue-2-articles/223-taxonomyforaminifera.

Mojtahid, M., Geslin, E., Coynel, A., Gorse, L., Vella, C., Davranche, A., Zozzolo, L., Blanchet, L., Bénéteau, E., Maillet, G., 2016. Spatial distribution of living (Rose Bengal stained) benthic foraminifera in the Loire estuary (western France). J. Sea Res. 118, 1–16. https://doi.org/10.1016/j.seares.2016.02.003

Murray, J.W., 2006. Ecology and Applications of Benthic Foraminifera. Cambridge University Press, Cambridge, 426 pp.

Parker, W.C., Arnold, A.J., 1999. Quantitative methods of analysis in foraminiferal ecology. In: Sen Gupta, B.K. (Ed.), Modern Foraminifera. Kluwer Academic Publishers, Dordrecht, pp. 71–89.

Pérez-Asensio, J.N., Aguirre, J., 2010. Benthic foraminiferal assemblages in temperate coral-bearing deposits from the late Pliocene. J. Foramin. Res. 40, 61–78. https://doi.org/10.2113/gsjfr.40.1.61

Pérez-Asensio, J.N., Aguirre, J., Schmiedl, G., Civis, J., 2012. Messinian paleoenvironmental evolution in the lower Guadalquivir Basin (SW Spain) based on benthic foraminifera. Palaeogeogr. Palaeoclimatol. Palaeoecol. 326–328, 135–151

555 Pérez-Asensio, J.N., Aguirre, J., Schmiedl, G., Civis, J., 2014. Messinian productivity
556 changes in the northeastern Atlantic and their relationship to the closure of the
557 Atlantic–Mediterranean gateway: implications for Neogene palaeoclimate and
558 palaeoceanography. J. Geol. Soc. London 171, 389–400.
559 https://doi.org/10.1144/jgs2013-032
560 Pérez-Asensio, J.N., Aguirre, J., Rodríguez-Tovar, F.J., 2017. The effect of bioturbation by
561 polychaetes (Opheliidae) on benthic foraminiferal assemblages and test preservation.
562 Palaeontology 60, 807–827. https://doi.org/10.1111/pala.12317
563 Pérez-Asensio, J.N., Frigola, J., Pena, L.D., Sierro, F.J., Reguera, M.I., Rodríguez-Tovar,
564 F.J., Dorador, J., Asioli, A., Kuhlmann, J., Huhn, K., Cacho, I., 2020. Changes in
565 western Mediterranean thermohaline circulation in association with a deglacial
566 Organic Rich Layer formation in the Alboran Sea. Quat. Sci. Rev. 228, 106075.
567 https://doi.org/10.1016/j.quascirev.2019.106075
568 Pérez-Ruzafa, A., De Pascalis, F., Ghezzo, M., Quispe-Becerra, J.I., Hernández-García, R.,
569 Muñoz, I., Vergara, C., Pérez-Ruzafa, I.M., Umgiesser, G., Marcos, C., 2019.
570 Connectivity between coastal lagoons and sea: Asymmetrical effects on assemblages'
571 and populations' structure. Estuar. Coast. Shelf Sci. 216, 171-186.
572 https://doi.org/10.1016/j.ecss.2018.02.031
573 Pethick, J., 1984. An Introduction to Coastal Geomorphology. Hodder Arnold Publication,
574 257 pp.
575 Reimer, P.J., Bard, E., Bayliss, A., Beck, J.W., Blackwell, P.G., Ramsey, C.B., Buck, C.E.,
576 Cheng, H., Edwards, R.L., Friedrich, M., Grootes, P.M., Guilderson, T.P., Haflidason,
577 H., Hajdas, I., Hatté, C., Heaton, T.J., Hoffmann, D.L., Hogg, A.G., Hughen, K.A.,
578 Kaiser, K.F., Kromer, B., Manning, S.W., Niu, M., Reimer, R.W., Richards, D.A.,
579 Scott, E.M., Southon, J.R., Staff, R.A., Turney, C.S.M., Plicht, J. van der, 2013.

IntCal13 and Marine13 Radiocarbon Age Calibration Curves 0–50,000 Years cal BP. Radiocarbon 55, 1869–1887. https://doi.org/10.2458/azu_js_rc.55.16947

Rich, V.I., Maier, R.M., 2015. Chapter 6 - Aquatic Environments, in: Pepper, I.L., Gerba, C.P., Gentry, T.J. (Eds.), Environmental Microbiology (Third Edition). Academic Press, San Diego, pp. 111–138. https://doi.org/10.1016/B978-0-12-394626-3.00006-5

Rodríguez-Ramírez, A., Yáñez-Camacho, C.M., 2008. Formation of chenier plain of the Doñana marshland (SW Spain): Observations and geomorphic model. Mar. Geol. 254, 187–196. https://doi.org/10.1016/j.margeo.2008.06.006

Rodríguez-Ramírez, A., Ruiz, F., Cáceres, L.M., Rodríguez Vidal, J., Pino, R., Muñoz, J.M., 2003. Analysis of the recent storm record in the southwestern Spanish coast: implications for littoral management. Sci. Total Environ. 303, 189–201. https://doi.org/10.1016/S0048-9697(02)00400-X

Rodríguez-Ramírez, A., Flores-Hurtado, E., Contreras, C., Villarías-Robles, J.J.R., Jiménez-Moreno, G., Pérez-Asensio, J.N., López-Sáez, J.A., Celestino-Pérez, S., Cerrillo-Cuenca, E., León, Á., 2014. The role of neo-tectonics in the sedimentary infilling and geomorphological evolution of the Guadalquivir estuary (Gulf of Cadiz, SW Spain) during the Holocene. Geomorphology 219, 126–140. https://doi.org/10.1016/j.geomorph.2014.05.004

Rodríguez-Ramírez, A., Pérez-Asensio, J.N., Santos, A., Jiménez-Moreno, G., Villarías-Robles, J.J.R., Mayoral, E., Celestino-Pérez, S., Cerrillo-Cuenca, E., López-Sáez, J.A., León, Á., Contreras, C., 2015. Atlantic extreme wave events during the last four millennia in the Guadalquivir estuary, SW Spain. Quat. Res. 83, 24–40. https://doi.org/10.1016/j.yqres.2014.08.005

Rodríguez-Ramírez, A., Villarías-Robles, J.J.R., Pérez-Asensio, J.N., Santos, A., Morales, J.A., Celestino-Pérez, S., León, Á., Santos-Arévalo, F.J., 2016. Geomorphological

record of extreme wave events during Roman times in the Guadalquivir estuary (Gulf of Cadiz, SW Spain): An archaeological and paleogeographical approach. Geomorphology 261, 103–118. https://doi.org/10.1016/j.geomorph.2016.02.030

Rodríguez-Ramírez, A., Villarías-Robles, J.J.R., Pérez-Asensio, J.N., Celestino-Pérez, S. 2019, The Guadalquivir Estuary: Spits and Marshes. In: Morales, J.A. (Ed.), The Spanish Coastal Systems. Springer, Switzerland, pp. 517–541.

Ruiz, F., González-Regalado, M.L., Borrego, J., Abad, M., Pendón, J.G., 2004. Ostracoda and foraminifera as short-term tracers of environmental changes in very polluted areas: the Odiel Estuary (SW Spain). Environ. Pollut. 129, 49–61. https://doi.org/10.1016/j.envpol.2003.09.024

Ruiz, F., González-Regalado, M.L., Pendón, J.G., Abad, M., Olías, M., Muñoz, J.M., 2005. Correlation between foraminifera and sedimentary environments in recent estuaries of Southwestern Spain: Applications to holocene reconstructions. Quat. Int. 140–141, 21–36. https://doi.org/10.1016/j.quaint.2005.05.002

Sen Gupta, B.K., Platon, E., 2006. Tracking past sedimentary records of oxygen depletion in coastal waters: USE of the *Ammonia–Elphidium* foraminiferal index. Journal of Coastal Research Special 39, 1331–1355.

Shepard F.P., 1954. Nomenclature based on sand-silt-clay ratios. Journal of Sedimentary Petrology 24, 151–158. https://doi.org/10.1306/D4269774-2B26-11D7-8648000102C1865D

Soares, A.M., 2015. Datación radiocarbónica de conchas marinas en el golfo de Cádiz: El efecto reservorio marino, su variabilidad durante el Holoceno e inferencias paleoambientales. Cuaternario y geomorfología 29, 19–29.

Spanish Ministry of Fomento, 2005. Información climática de nivel del mar. Mareógrafo de Sevilla (Bonanza), 6 pp.

630 Stuiver, M., Reimer, P.J., 1993. Extended ^{14}C Data Base and Revised CALIB 3.0 ^{14}C Age
631 Calibration Program. Radiocarbon 35, 215–230.
632 https://doi.org/10.1017/S0033822200013904
633 Vaiani, S.C., 2000. Testing the applicability of strontium isotope stratigraphy in marine to
634 deltaic Pleistocene deposits: An example from the Lamone River Valley (Northern
635 Italy). J. Geol. 108, 585–599. https://doi.org/10.1086/314416
636 Vanney, J.R., 1970. L'hydrologie du Bas Guadalquivir. CSIC, Departamento de Geografía
637 Aplicada, Madrid.
638 Wukovits, J., Oberrauch, M., Enge, A.J., Heinz, P., 2018. The distinct roles of two intertidal
639 foraminiferal species in phytodetrital carbon and nitrogen fluxes—Results from
640 laboratory feeding experiments. Biogeosciences 15, 6185–6198.
641 https://doi.org/10.5194/bg-15-6185-2018
642 Ybert, J.-P., Bissa, W.M., Catharino, E.L.M., Kutner, M., 2003. Environmental and sea-level
643 variations on the southeastern Brazilian coast during the Late Holocene with
644 comments on prehistoric human occupation. Palaeogeogr. Palaeoclimatol. Palaeoecol.
645 189, 11–24. https://doi.org/10.1016/S0031-0182(02)00590-4
646

647 **Figure captions**

648 **Figure 1.** Study area and location of the short and deep cores. The Spanish local term ‘caño’
649 refers to a relict, fully filled-in tidal-fluvial channel. Upper map created with GeoMapApp
650 (http://www.geomapapp.org/). (For interpretation of the references to colour in this figure
651 legend, the reader is referred to the Web version of this article).

652

653 **Figure 2.** Lithostratigraphy, chronology and benthic foraminiferal data (dominant species %,
654 BFS index) of the short and deep cores. (For interpretation of the references to colour in this
655 figure legend, the reader is referred to the Web version of this article).

656

657 **Figure 3.** Principal Component (PC) scores of the dominant euryhaline benthic foraminiferal
658 species of the short and deep cores. (For interpretation of the references to colour in this
659 figure legend, the reader is referred to the Web version of this article).

660

661 **Figure 4.** Benthic foraminiferal Salinity index values (BFS index) of the short and deep cores
662 showing the Holocene paleoenvironmental evolution of the Guadalquivir estuary. (For
663 interpretation of the references to colour in this figure legend, the reader is referred to the
664 Web version of this article).

665

666 **Figure 5.** Comparison of the Benthic Foraminiferal Salinity index values (BFS index) of
667 three marginal-marine environments from different regions and timescales: core S7 (this
668 study), core 223 S12 (Barbieri and Vaiani, 2018), and Rambla de la Sepultura (RS) section
669 (Pérez-Asensio and Aguirre, 2010) (For interpretation of the references to colour in this
670 figure legend, the reader is referred to the Web version of this article).

671

672 **Table captions**

673 **Table 1.** Location (latitude, longitude) of the studied short and long cores (S6, LB, AR, AA,
674 VT, VAc, VAli.2 VAli.1, S7, S11).

675

676 **Table 2.** Radiocarbon ^{14}C data using the CALIB 7.10 software (Stuiver and Reimer, 1993),
677 the calibration dataset of Reimer et al. (2013), and a ΔR value of −108 ± 31 ^{14}C yr (Soares,
678 2015). Uncertainties of the calibrated ages are expressed as 2σ errors. B.—Beta Analytic
679 Laboratory (Miami, USA). CNA.—Centro Nacional de Aceleradores (Seville, Spain).
680 DAMS.—Accium BioSciences Accelerator Mass Spectrometry Lab (Seattle, USA). CX.—
681 Geochron Laboratories, Krueger Enterprises, Inc. (Cambridge, USA). (1) Rodríguez-Ramírez
682 et al. (2014). (2) Rodríguez-Ramírez et al. (2015). (3) Rodríguez-Ramírez et al. (2016).

683

684 **Table 3.** Q-mode principal component analysis results from the short and deep cores.
685 Explained variance (%) of each PC axis (assemblage), and the dominant and secondary
686 species are indicated.

687

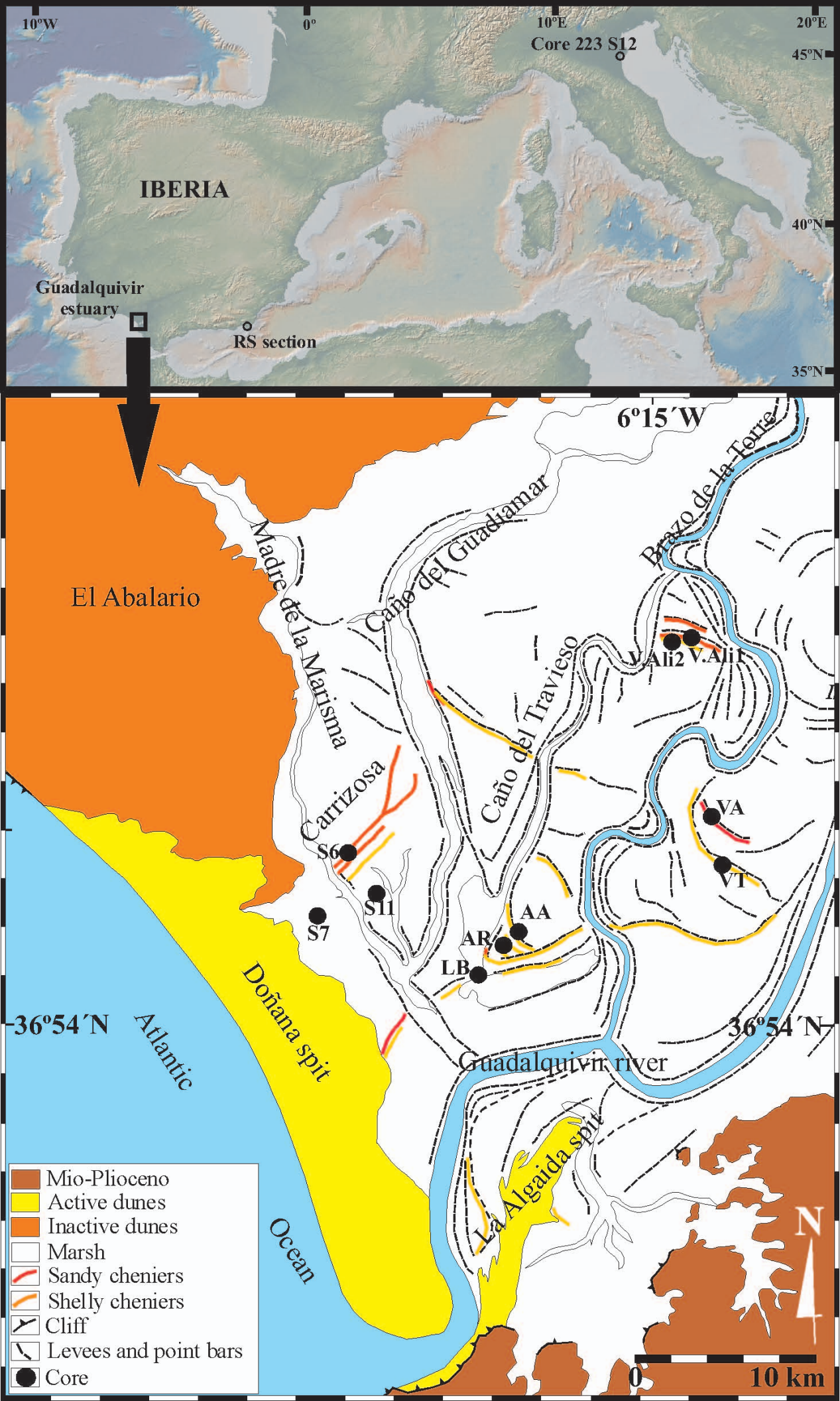
10°W
0°
10°E
20°E
45°N
40°N
35°N
Core 223 S12
IBERIA
Guadalquivir estuary
RS section
6°15´W
El Abalario
Madre de la Marisma
Caño del Guadiamar
Brazo de la Torre
Caño del Travieso
V.Ali2
V.Ali1
Carrizosa
S6
S11
S7
VA
VT
AA
AR
LB
Doñana spit
36°54´N
Atlantic
Ocean
Guadalquivir river
La Algaida spit
N
0
10 km
Mio-Plioceno
Active dunes
Inactive dunes
Marsh
Sandy cheniers
Shelly cheniers
Cliff
Levees and point bars
Core

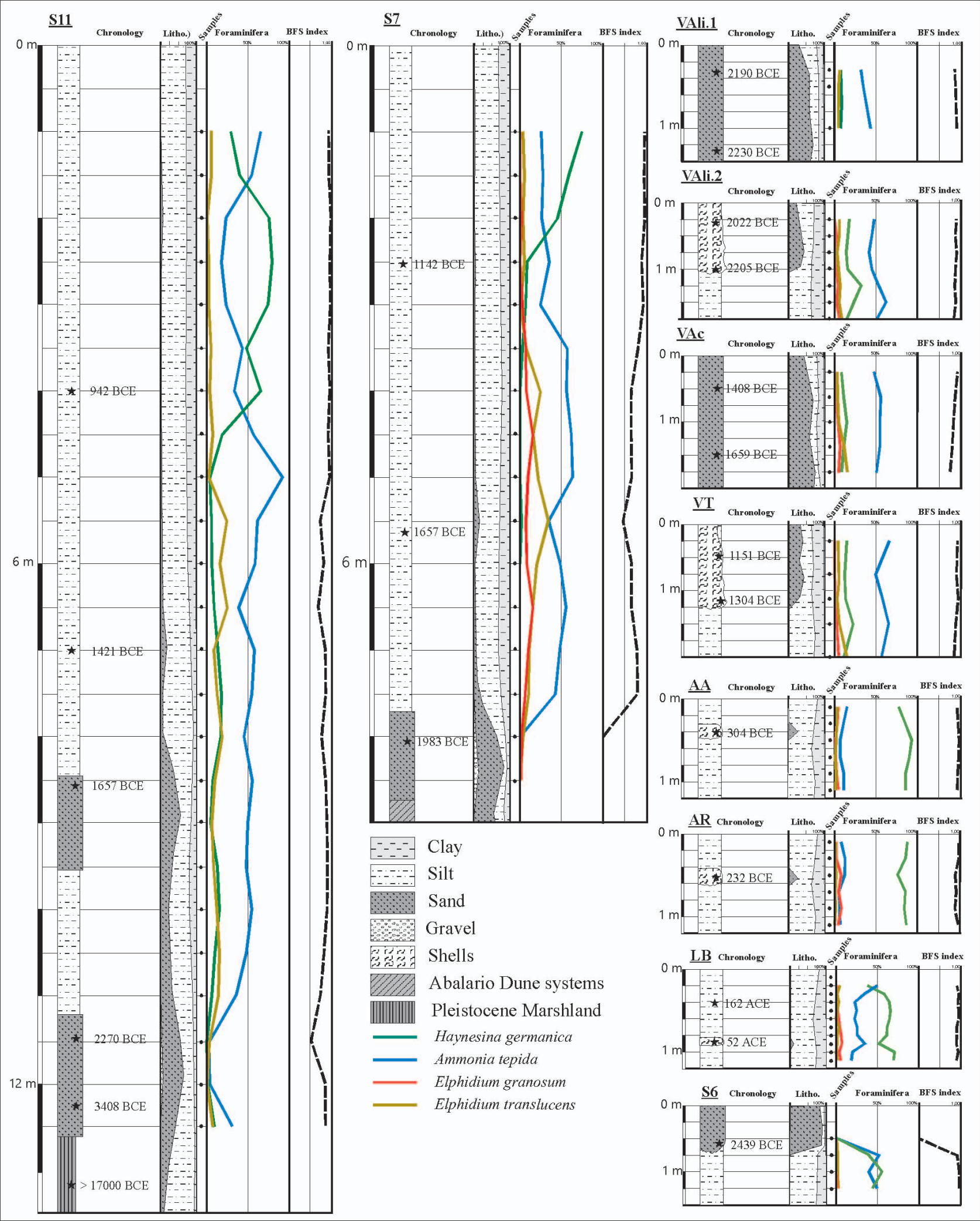
S11
Chronology
Litho.)
Samples
Foraminifera
BFS index
0 m
6 m
12 m
942 BCE
1421 BCE
1657 BCE
2270 BCE
3408 BCE
> 17000 BCE
S7
1142 BCE
1657 BCE
1983 BCE
Clay
Silt
Sand
Gravel
Shells
Abalario Dune systems
Pleistocene Marshland
Haynesina germanica
Ammonia tepida
Elphidium granosum
Elphidium translucens
VAli.1
2190 BCE
2230 BCE
VAli.2
2022 BCE
2205 BCE
VAc
1408 BCE
1659 BCE
VT
1151 BCE
1304 BCE
AA
304 BCE
AR
232 BCE
LB
162 ACE
52 ACE
S6
2439 BCE
1 m

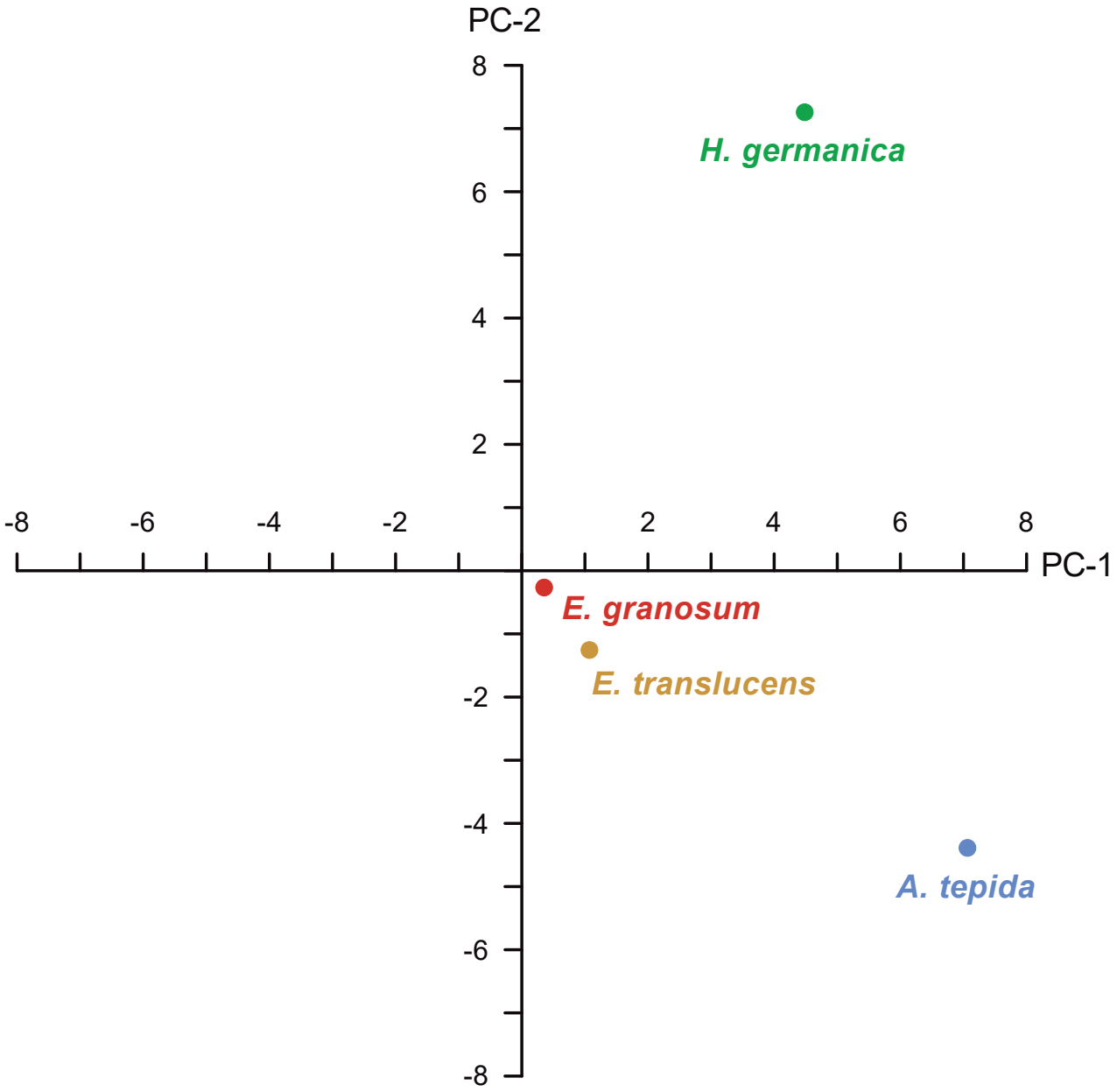
PC-2
8
6
4
2
-8
-6
-4
-2
2
4
6
8
PC-1
-2
-4
-6
-8
H. germanica
E. granosum
E. translucens
A. tepida

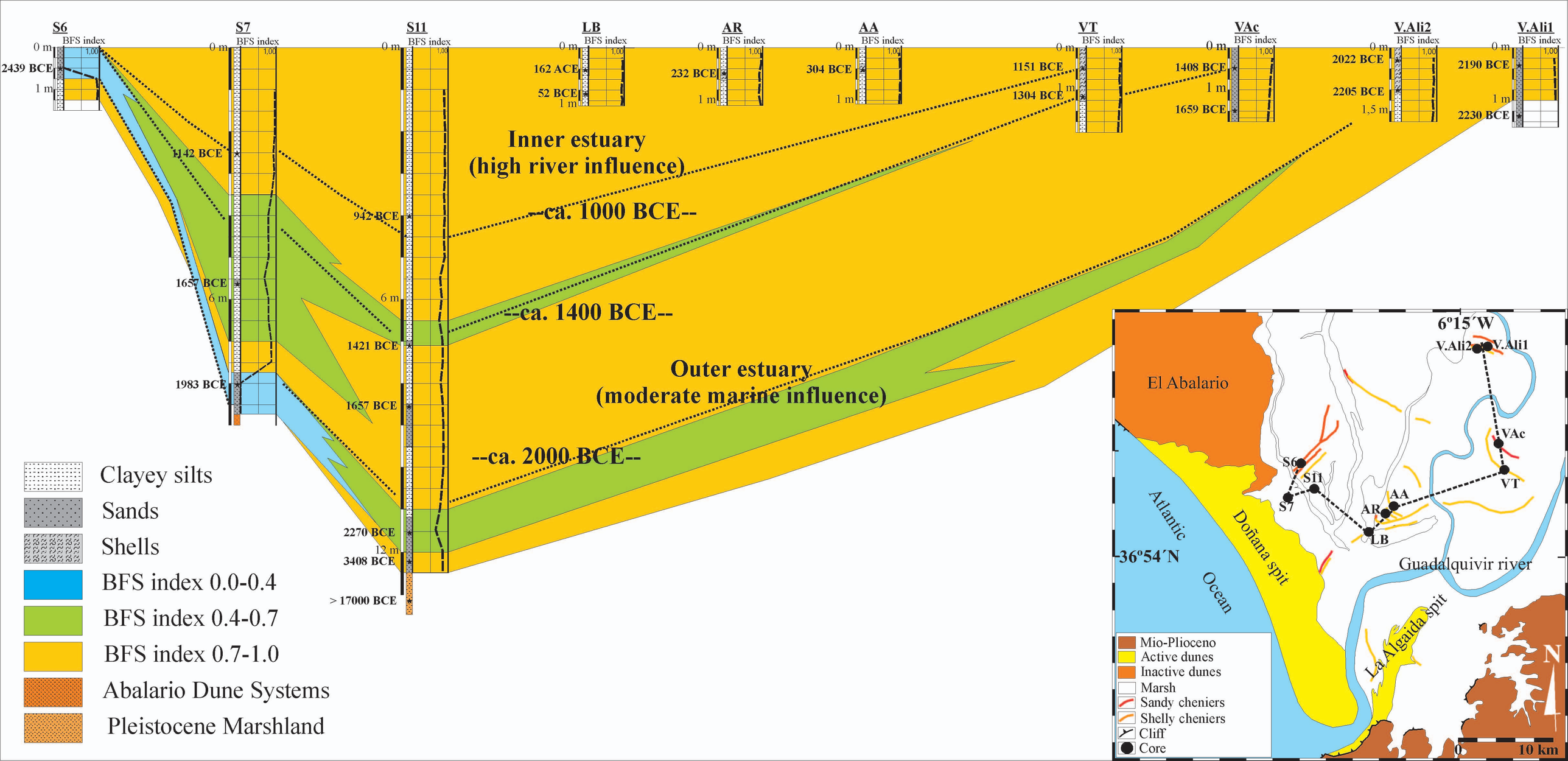
S6
S7
S11
LB
AR
AA
VT
VAc
V.Ali2
V.Ali1
BFS index
0 m
1,00
2439 BCE
1 m
142 BCE
1657 BCE
6 m
1983 BCE
942 BCE
1421 BCE
1657 BCE
2270 BCE
12 m
3408 BCE
> 17000 BCE
162 ACE
52 BCE
232 BCE
304 BCE
1151 BCE
1304 BCE
1408 BCE
1659 BCE
2022 BCE
2205 BCE
1,5 m
2190 BCE
2230 BCE
Inner estuary
(high river influence)
--ca. 1000 BCE--
--ca. 1400 BCE--
Outer estuary
(moderate marine influence)
--ca. 2000 BCE--
Clayey silts
Sands
Shells
BFS index 0.0-0.4
BFS index 0.4-0.7
BFS index 0.7-1.0
Abalario Dune Systems
Pleistocene Marshland
6º15´W
36º54´N
El Abalario
Atlantic
Ocean
Doñana spit
La Algaida spit
Guadalquivir river
Mio-Plioceno
Active dunes
Inactive dunes
Marsh
Sandy cheniers
Shelly cheniers
Cliff
Core
N
0
10 km

2.5 pt

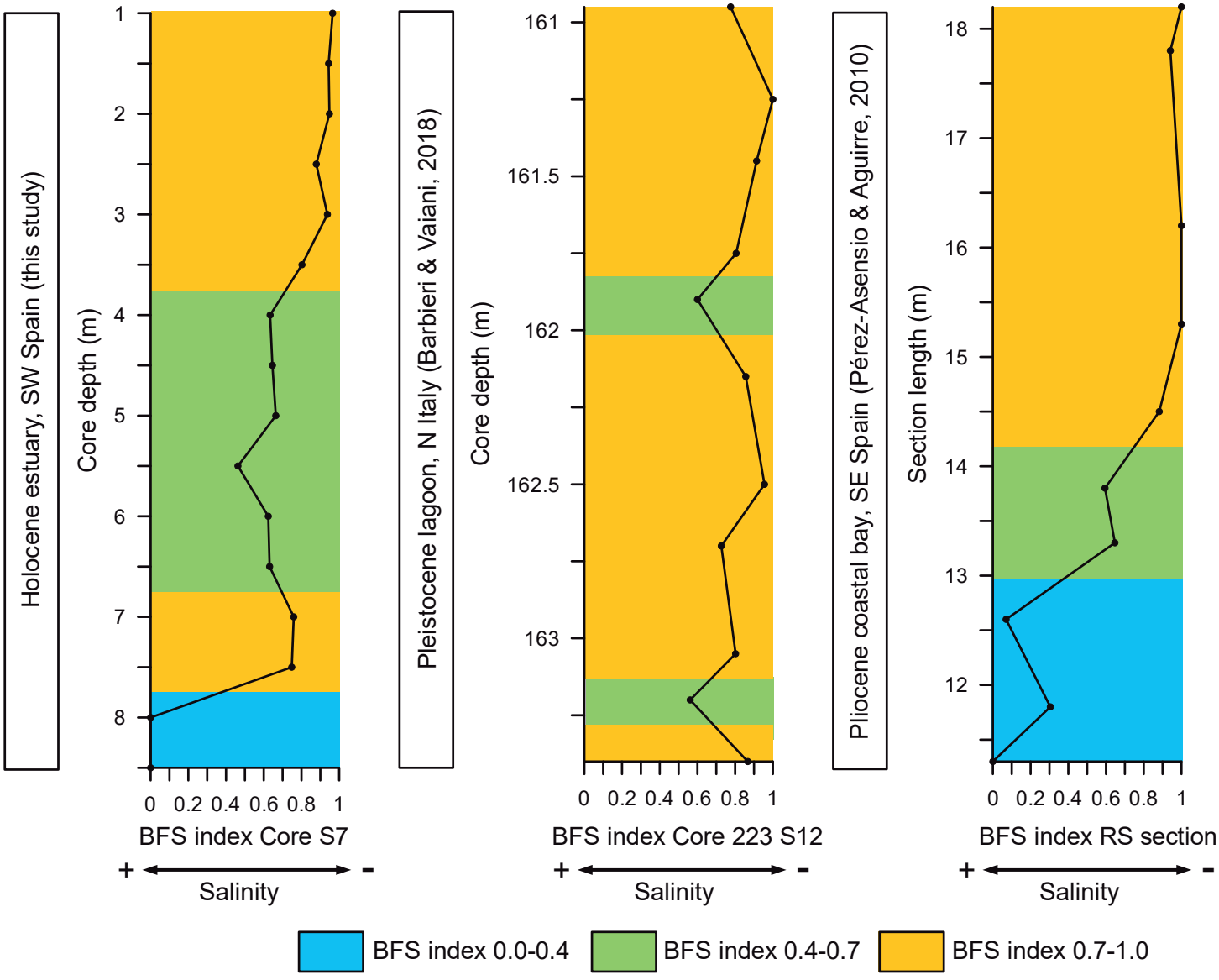
Holocene estuary, SW Spain (this study)
Core depth (m)
1
2
3
4
5
6
7
8
0 0.2 0.4 0.6 0.8 1
BFS index Core S7
+
-
Salinity
Pleistocene lagoon, N Italy (Barbieri & Vaiani, 2018)
Core depth (m)
161
161.5
162
162.5
163
0 0.2 0.4 0.6 0.8 1
BFS index Core 223 S12
+
-
Salinity
Pliocene coastal bay, SE Spain (Pérez-Asensio & Aguirre, 2010)
Section length (m)
18
17
16
15
14
13
12
0 0.2 0.4 0.6 0.8 1
BFS index RS section
+
-
Salinity
BFS index 0.0-0.4
BFS index 0.4-0.7
BFS index 0.7-1.0

Core	Latitude	Longitude
S6	36º58´35.90˝N	6º24´39.08˝W
LB	36º56´24.95˝N	6º20´04.55˝W
AR	36º56´47.99˝N	6º19´15.98˝W
AA	36º56´56.67˝N	6º19´05.50˝W
VT	36º58´00.78˝N	6º13´04.52˝W
VAc	36º59´38.31˝N	6º13´07.99˝W
VAli.2	37º04´13.89˝N	6º14´19.84˝W
VAli.1	37º04´13.37˝N	6º14´27.25˝W
S7	36º56´27.79˝N	6º24´46.46˝W
S11	36º58´04.93˝N	6º23´47.38˝W

Core	Lab. Ref.	Depth (m)	^{14}C age (BP)	^{14}C cal yr 2σ (BCE-ACE)
S6	B-287646[1]	-0.5	4370±40	2757 BCE-(2439BCE)-2122 BCE
S7	B-285000[2]	-2.5	3370±40	1409BCE-(1142BCE)-876BCE
S7	B-285001[2]	-5.5	3780±40	1917BCE-(1657BCE)-1397BCE
S7	B-285002[2]	-8	4040±40	2281BCE-(1983BCE)-1685BCE
S11	B-285006[2]	-4	3190±40	1244BCE-(942BCE)-722BCE
S11	D-AMS 002422[2]	-7	3596±60	1719BCE-(1421BCE)-1123BCE
S11	D-AMS 001537[2]	-8.5	3781±33	1912BCE-(1657BCE)-1402BCE
S11	D-AMS 001538[2]	-11.5	4260±30	2560BCE -(2270BCE)-1981BCE
S11	B-285007[2]	-12.5	4860±40	3511BCE-(3408BCE)-3305BCE
S11	B-285008[2]	-13.5	19360±80	Uncalibrated
VAli.1	D-AMS 030336	-1.3	4226±68	2557BCE-(2230BCE)-1904BCE
VAli.1	D-AMS 013505	0.4	4200±27	2470BCE-(2190BCE)-1910BCE
VAli.2	D-AMS 013507	0.5	4067±27	2314 BCE-(2022BCE)-1730 BCE
VAli.2	D-AMS 013506	-0.75	4215±24	2486 BCE-(2205BCE)-1925 BCE
VAc	CNA1118	-0.5	3590±80	1737 BCE-(1408BCE)-1079 BCE
VAc	DAMS-002424[2]	-1.5	3778±54	1937 BCE-(1659BCE)-1382 BCE
VT	D-AMS 030340	-0.5	3384±64	1442 BCE-(1151BCE)-860 BCE
VT	CNA1117[2]	-1.1	3504±48	1589 BCE-(1304BCE)-1019 BCE
AA	D-AMS 008483[3]	-0.5	2494± 23	413 BCE-(304BCE)-196 BCE
AR	D-AMS 008481[3]	-0.5	2404± 27	351 BCE-(232BCE)-113 BCE
LB	D-AMS 030339	-0.5	1981±60	113ACE-(162ACE)-437ACE
LB	D-AMS 008482	-0.8	2267± 26	166 BCE-(52ACE)-62 ACE

PC	Variance (%)	Species	Score
1	67.8	*Ammonia tepida*	7.06
		Haynesina germanica	4.48
		Elphidium translucens	1.07
		Elphidium granosum	0.35
2	23.3	*Haynesina germanica*	7.26
3	4.2	*Triloculina trigonula*	7.48
		Ammonia beccarii	2.76
		Quinqueloculina seminula	1.58
		Miliolinella sp.	1.14
		Quinqueloculina sp.	1.12
		Triloculina sp.	0.76
		Quinqueloculina vulgaris	0.53
		Quinqueloculina laevigata	0.45